Radiology Case Reports 18 (2023) 3626–3631

Available online at www.sciencedirect.com

ScienceDirect

journal homepage: www.elsevier.com/locate/radcr

Case Report

Magnetic resonance imaging findings of sclerosing microcystic adenocarcinoma: A case report and review of the literature ☆

Hiroyuki Fujii, MD, PhD[a,*], *Tadahide Noguchi, DDS, PhD*[b], *Tamaki Miura, MD*[c], *Nana Fujii, MD*[a], *Takenori Isozaki, MD*[a], *Akifumi Fujita, MD, PhD*[d], *Toshiro Niki, MD, PhD*[c], *Mitsuru Matsuki, MD, PhD*[a], *Harushi Mori, MD, PhD*[a]

[a] *Department of Radiology, Jichi Medical University, Tochigi, Japan*
[b] *Department of Dentistry, Oral and Maxillofacial Surgery, Jichi Medical University, Tochigi, Japan*
[c] *Department of Integrative Pathology, Jichi Medical University, Tochigi, Japan*
[d] *Department of Radiology, Haga Red Cross Hospital, Tochigi, Japan*

ARTICLE INFO

Article history:
Received 25 May 2023
Revised 13 July 2023
Accepted 21 July 2023

Keywords:
Sclerosing microcystic adenocarcinoma
Microcystic adnexal carcinoma
Salivary gland
MRI

ABSTRACT

Sclerosing microcystic adenocarcinoma (SMA) is a rare malignant tumor of the salivary glands that closely resembles cutaneous microcystic adnexal carcinoma (MAC). It was newly listed in the 5th edition of the WHO classification of head and neck tumors. This report describes the case of a 61-year-old woman who presented with masses on the floor of the mouth. The masses showed low signal intensity on T2-weighted images (T2WI) and with low apparent diffusion coefficient (ADC) values. Dynamic contrast-enhanced magnetic resonance imaging (DCE-MRI) revealed a plateau or persistence after rapid initial enhancement. Histopathologically, the tumors comprised small infiltrating strands of cells that formed small ducts and cysts embedded in thick fibrous stroma, consistent with SMA. Low signal intensity on T2WI with a low ADC value and a plateau or persistence after rapid initial enhancement on DCE-MRI reflect the fibrous and cellular components of the tumor and can be considered characteristic MRI findings of SMA.

Abbreviations: SMA, sclerosing microcystic adenocarcinoma; MAC, microcystic adnexal carcinoma; MRI, magnetic resonance imaging; T1WI, T1-weighted image; T2WI, T2-weighted image; DWI, diffusion-weighted image; ADC, apparent diffusion coefficient; DCE-MRI, dynamic contrast-enhanced magnetic resonance imaging; CEA, carcinoembryonic antigen; EMA, epithelial membrane antigen.

☆ Competing Interests: The authors declare that they have no known competing financial interests or personal relationships that could have appeared to influence the work reported in this paper.

* Corresponding author.
E-mail address: hiroyuki.fujii@jichi.ac.jp (H. Fujii).

https://doi.org/10.1016/j.radcr.2023.07.050

Introduction

Microcystic adnexal carcinoma (MAC) is an uncommon cutaneous tumor that exhibits ductal and follicular differentiation [1]. MAC is an indolent, locally aggressive, and deeply infiltrative tumor with a high propensity for perineural invasion [2,3] and is most common in the head and neck region [1]. MAC rarely occurs in extracutaneous locations, including the oral cavity and other mucosal head and neck regions where adnexal keratinocytes do not exist [4–10]. In 2016, Mills et al. proposed the term "sclerosing microcystic adenocarcinoma (SMA)" for a rare malignant tumor occurring in the salivary glands, closely resembling cutaneous MAC [11]. To our knowledge, 21 cases of SMA have been reported, but none have evaluated the magnetic resonance imaging (MRI) findings of SMA in detail [4–18]. Here, we report an additional case of SMA of the floor of the mouth and discuss its MRI findings.

Case report

A 61-year-old woman presented to our hospital with a mass on the left side of the floor of the mouth. The patient was asymptomatic and had a history of multiple MACs, for which she underwent surgical resection of a right eyelid lesion and left frontal lesion at the ages of 51 and 58, respectively. The patient had no relevant medical history. On intraoral examination, a mass of approximately 1 cm in size was palpated on the left floor of the mouth (Fig. 1a) and hard tissue resembling a salivary stone was detected on the right floor of the mouth (Fig. 1b). Laboratory findings were unremarkable.

An orthopantomogram showed no obvious abnormalities. MRI revealed a 10-mm, partially ill-defined mass in the left sublingual gland (Fig. 2) and a 7-mm mass in the right sublingual gland (Fig. 3). The masses showed isointensity to muscle on T1-weighted images (T1WI), iso to slightly higher signal intensity to muscle on T2-weighted images (T2WI), and low signal intensity on the apparent diffusion coefficient (ADC) map derived from diffusion-weighted images ($b = 1000$ s/mm^2). The ADC value of the right sublingual gland lesion was 0.88×10^{-3} mm/s and that of the right sublingual lesion was 1.20×10^{-3} mm/s. On dynamic contrast-enhanced MRI (DCE-MRI), the left sublingual lesion showed rapid initial enhancement, followed by a period of continuous enhancement at a slower rate. The right sublingual lesion showed rapid initial enhancement before reaching a plateau. Contrast-enhanced fat-suppressed T1WI showed a uniform iso- to slightly stronger enhancement than the surrounding normal sublingual gland.

A follow-up MRI performed after 4 months showed no significant changes. Excisional biopsy was performed for diagnostic and therapeutic purposes. The mass in the left sublingual gland showed strong adhesions to the surrounding tissues, particularly the mylohyoid muscle and lingual nerve. The mass in the right sublingual gland also showed adhesions to the surrounding tissues but to a lesser degree than that on the left side.

Histopathologically, the tumors comprised small infiltrating strands of cells forming small ducts and cysts with mild atypia and were embedded in thick fibrous stroma (Fig. 4a). Preexisting sublingual gland tissue was observed in the marginal zone of the tumors. Tumor cells were scattered within the peripheral nerves and along the perineurium, indicative of a perineural invasion. Immunohistological findings were positive for cytokeratin 7, carcinoembryonic antigen (CEA), and epithelial membrane antigen (EMA) (Fig. 4b–d). Although these findings were consistent with those for MAC and SMA, a diagnosis of SMA was favored because the masses were situated in locations where adnexal keratinocytes were absent. Imaging and intraoperative findings also suggested that the tumors originated from the sublingual gland.

The patient received postoperative intensity-modulated radiation therapy at 60 Gy in 30 fractions. The postoperative course was uneventful, and no recurrence or distant metastases were identified at the 21-month follow-up after surgery.

Discussion

This report describes a case of SMA on the floor of the mouth. The term SMA was proposed in 2016 by Mills et al. [11] for a rare malignant tumor occurring in the salivary glands, closely resembling a cutaneous MAC. SMA has previously been

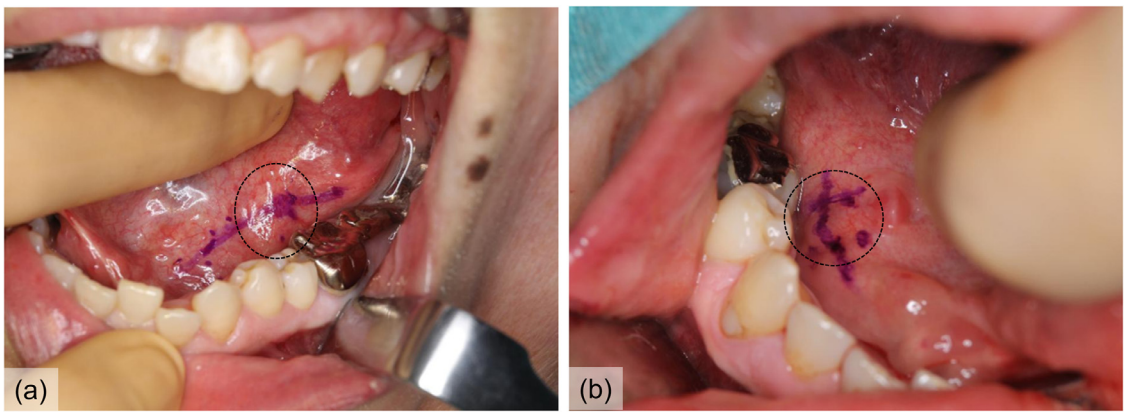

Fig. 1 – Intraoral findings of masses on the left (a, dotted circle) and right (b, dotted circle) sides of the floor of the mouth.

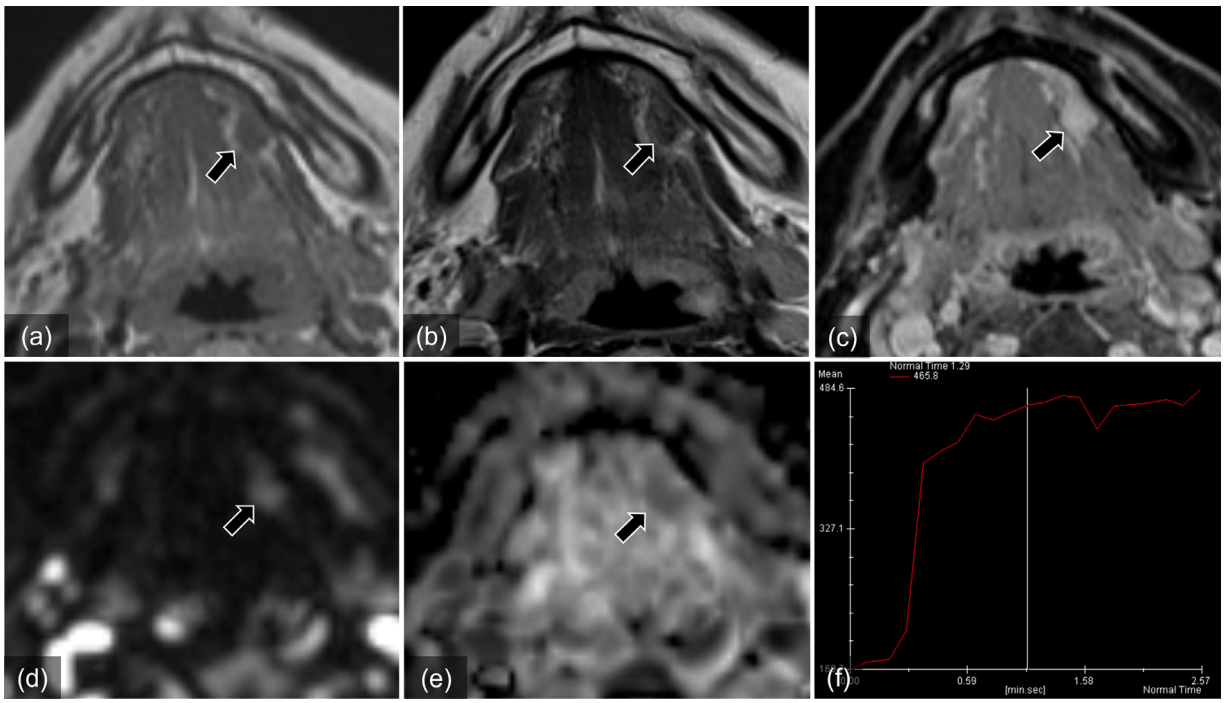

Fig. 2 – Magnetic resonance images of the mass on the left side of the floor of the mouth. (a) axial T1-weighted image (T1WI), (b) axial T2-weighted image (T2WI), (c) axial contrast-enhanced fat-suppressed T1WI, (d) axial diffusion-weighted image (DWI) (b = 1000 s/mm^2), (e) apparent diffusion coefficient (ADC) map, (f) time–intensity curve of dynamic contrast-enhanced MRI. The mass shows isointensity relative to the surrounding muscle on T1WI (a, arrow), a heterogeneous low signal on T2WI (b, arrow), high signal intensity on DWI (d, arrow), and low signal intensity on the ADC map (e, arrow). The time–intensity curve shows a rapid initial enhancement, followed by a period of continuous enhancement at a slower rate (f). The mass shows uniform enhancement (c, arrow).

termed oral MAC, sclerosing sweat duct-like carcinoma, and syringomatous adenocarcinoma [5–10]. SMA is now recognized as a distinct salivary gland malignancy and was included for the first time in the fifth edition of the WHO classification of head and neck tumors [19].

Table 1 summarizes the characteristics of the previously reported cases of SMA and the present patient. In total, 22 cases were reviewed. The male-to-female ratio was 6:16, and the median age was 54.5 years (range, 41-73 years). The most common primary site was the tongue (n = 10), followed by the floor of the mouth (n = 4). Other reported sites included the lips (n = 2), buccal mucosa (n = 2), palate (n = 1), nasopharynx (n = 1), and parotid gland (n = 2). Contrary to MAC, which originates from eccrine sweat glands and is localized to the skin, SMA occurs on the nonadnexal mucosal surfaces of the head and neck region and is purported to have a salivary gland origin. Although follow-up data are limited, SMA has been reported to have a better prognosis than cutaneous MAC, with no reports of local recurrence or metastasis to date.

Histopathologically, SMA consists of deeply infiltrative nests, cords, and tubules of tumor cells embedded in prominent desmoplastic to densely collagenous stroma, similar to cutaneous MAC [20]. The tumor is biphasic, with bland luminal cuboidal ductal cells having an eosinophilic or clear cytoplasm and flat peripheral myoepithelial cells. Nuclei are bland and round to oval in shape, with occasional nucleoli. The ducts contain focal eosinophilic secretions. Mitotic figures were not conspicuous. Perineural invasion is commonly observed. Lesion cells stain with antibodies against CEA, EMA, and AE1/3, although the immunohistochemistry is nonspecific and morphological diagnosis remains the gold standard [12].

To our knowledge, no study has conducted a detailed review of the MRI findings of SMA. Among the 21 reported cases of SMA, imaging findings were described in 4, as follows: computed tomography (CT) (n = 2), 18F-fluorodeoxyglucose-positron emission tomography/CT (18F-FDG-PET/CT) (n = 1), and MRI (n = 2) [11,13,17,18]. As these reports did not describe the imaging findings of the SMA in detail, we reviewed the available images and summarized the findings as follows. On CT, the SMA had ill-defined borders and showed isodensity with the surrounding muscle [13,18]. The lesion showed high uptake of FDG on 18F-FDG-PET/CT (standardized uptake value not stated) [18]. MRI findings revealed an iso-signal intensity to muscle on T2WI with gadolinium enhancement [11,17]. Consistent with the findings of previous studies, the lesions, in this case, were visualized as partially ill-defined masses with iso to slightly higher signal intensity than the surrounding muscle on T2WI and uniform gadolinium enhancement. Based on the histological findings, a low signal intensity on T2WI with a low ADC value reflects a densely collagenous stroma and abundant cellular components. A densely collagenous stroma reduces the signal intensity on T2WI, whereas

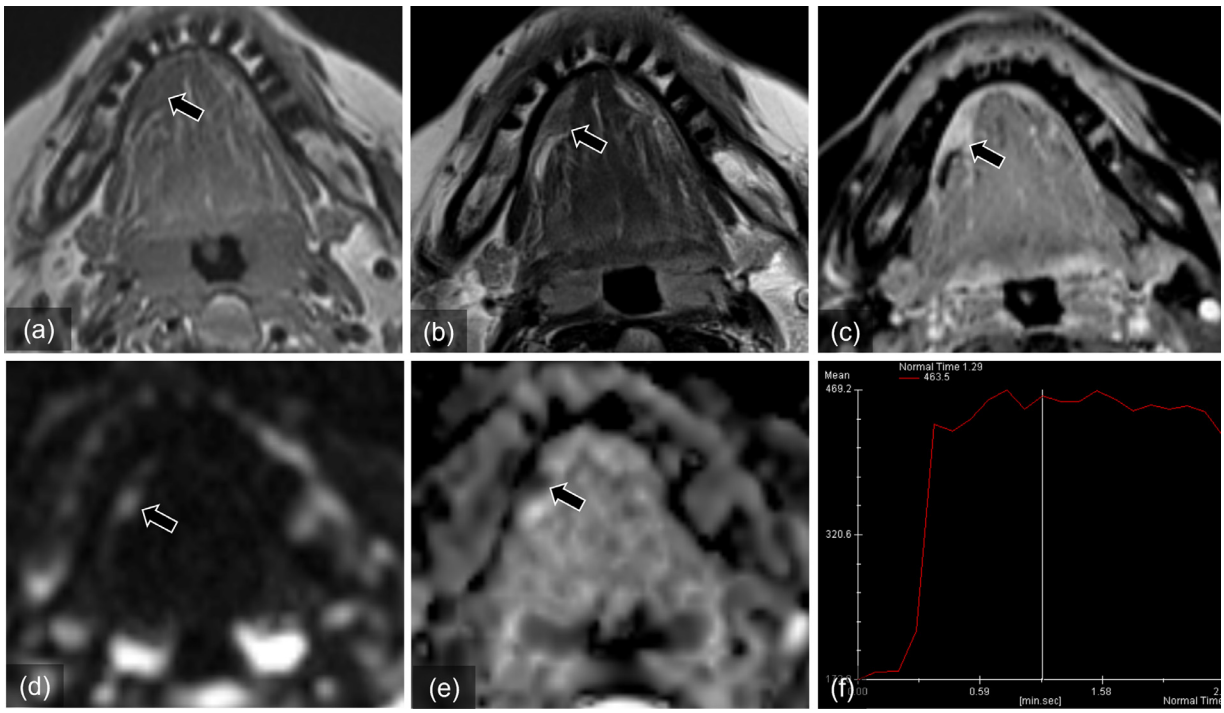

Fig. 3 – Magnetic resonance images of the mass on the right side of the floor of the mouth. (a) axial T1-weighted image (T1WI), (b) axial T2-weighted image (T2WI), (c) axial contrast-enhanced fat-suppressed T1WI, (d) axial diffusion-weighted image (DWI) (b = 1000 s/mm^2), (e) apparent diffusion coefficient (ADC) map, (f) time–intensity curve of dynamic contrast-enhanced MRI. The mass shows isointensity relative to the surrounding muscle on T1WI, homogenous hypointensity on T2WI, and restricted diffusion (a, b, d, e, arrows). The time–intensity curve shows a rapid initial enhancement before reaching a plateau. (f) The mass shows uniform, slightly stronger enhancement than the normal sublingual gland (c, arrow).

Table 1 – Summary of known cases of sclerosing microcystic adenocarcinoma.

Case	Author [reference]	Age (y)	Sex	Location	Imaging findings	Treatment	Follow up data (months)
1	Johnstone & Toker [4]	67	F	Mid lower lip	Not stated	Excision	Disease free (36)
2	Johnstone & Toker [4]	57	F	Upper lip	Not stated	Excision	Disease free (16)
3	Bondi et al. [5]	71	F	Cheek	Not stated	Excision	Disease free (7)
4	Schipper et al. [6]	65	M	Tongue	Not stated	Radiotherapy	No change in tumor size (21)
5	Closmann & Torske [7]	43	M	Cheek	Not stated	Excision	Not stated
6	Petersson et al. [8]	70	F	Left posterior tongue	Not stated	Excision and adjuvant radiotherapy	Disease free (21)
7	Basile et al. [9]	53	F	Tongue	Not stated	Not stated	Not stated
8	Ide at al. [10]	52	F	Palate	Not stated	Excision	Disease free (48)
9	Mills et al. [11]	41	F	Tongue base	Not stated	Not stated	Not stated
10	Mills et al. [11]	47	F	Tongue	Not stated	Not stated	Not stated
11	Mills et al. [11]	73	F	Nasopharynx	MRI	Not stated	Not stated
12	Mills et al. [11]	54	M	Floor of mouth	Not stated	Not stated	Not stated
13	Mills et al. [11]	48	F	Floor of mouth	Not stated	Chemoradiotherapy	Disease free (24)
14	Wood et al. [12]	68	F	Tip of tongue	Not stated	Excision	Disease free (60)
15	Wood et al. [12]	49	F	Right lateral tongue	Not stated	Excision	Disease free (14)
16	Zhang et al. [13]	55	F	Floor of mouth	CT	Excision and adjuvant radiotherapy	Disease free (10)
17	Zhang et al. [14]	51	M	Tongue	Not stated	Excision	Disease free (38)
18	Jiang et al. [15]	41	F	Tongue	Not stated	Excision	Not stated
19	Tan et al. [16]	73	M	Left parotid gland	Not stated	Excision	Disease free (4)
20	Elizabath et al. [17]	67	F	Right parotid gland	MRI	Excision and adjuvant radiotherapy	Disease free (6)
21	Lee et al. [18]	48	M	Tongue	FDG-PET/CT	Excision	Disease free (30)
22	Present case	61	F	Floor of mouth	MRI	Excision and adjuvant radiotherapy	Disease free (21)

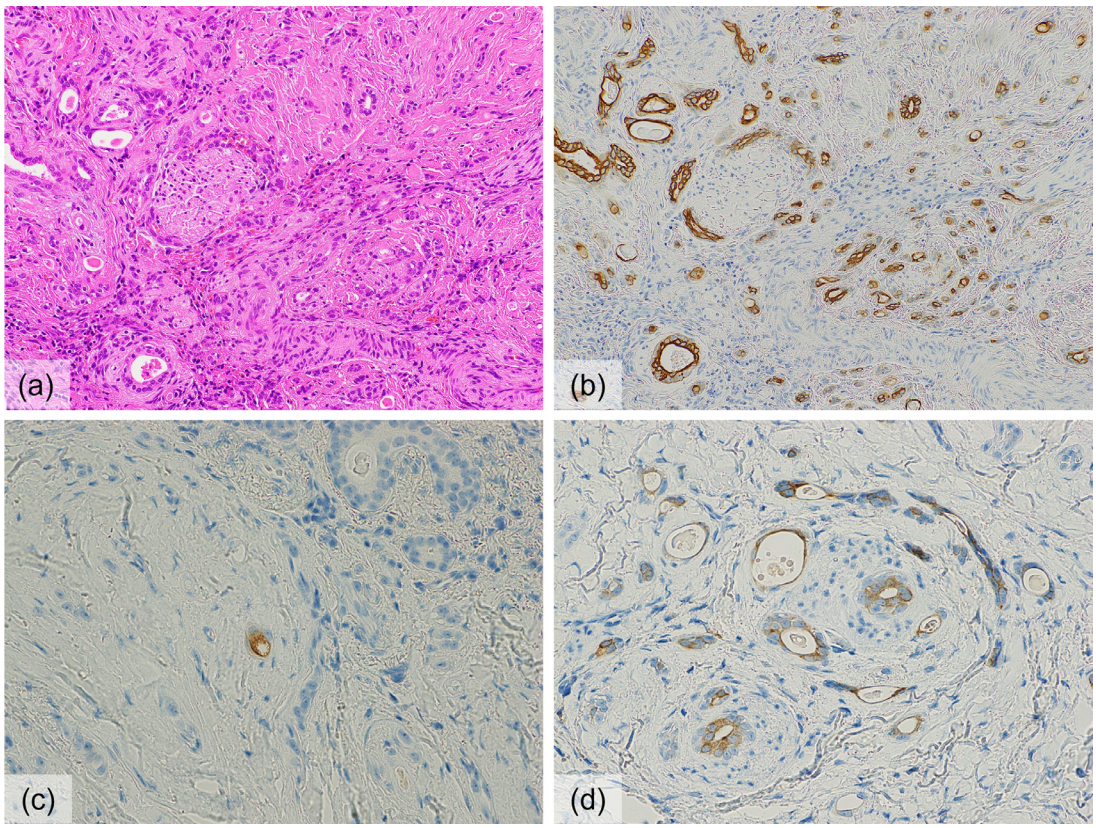

Fig. 4 – Histopathological findings. (a) hematoxylin-eosin staining, (b) cytokeratin 7 (CK7) staining, (c) carcinoembryonic antigen (CEA) staining, and (d) epithelial membrane antigen (EMA) staining. The tumors are composed of small infiltrating strands of cells forming small ducts and cysts with mild atypia and are embedded in thick fibrous stroma (a). Immunohistological findings are positive for CK7, CEA, and EMA, consistent with microcystic adnexal carcinoma or sclerosing microcystic adenocarcinoma (b–d).

abundant cellular components decrease the ADC value. In addition, DCE-MRI showed a plateau or persistent signal intensity after the initial rapid enhancement, which reflects the collagenous stroma of the tumor. Therefore, low signal intensity on T2WI with a low ADC value and a plateau or persistence of signal intensity after initial rapid enhancement on DCE-MRI can be considered characteristic MRI findings of SMA. To date, only 1 case report has described the imaging findings of cutaneous MAC [21], which showed low signal intensity and was isointense to the muscles, similar to those reported for SMA. We believe that the imaging similarities between cutaneous MAC and SMA reflect their pathological similarities.

Because the patient had a history of multiple MACs, it is important to evaluate whether the lesions on the floor of the mouth were metastases of MAC to the sublingual glands. We believe that these were primary lesions rather than metastatic lesions for 2 reasons. First, metastasis to the sublingual gland is extremely rare, with only 1 case (of renal cancer) reported to date [22,23]. Furthermore, bilateral sublingual gland metastases are rarer. Second, we reviewed the patient's past imaging findings and found that the sublingual gland masses were confirmed using MRI at the age of 54, between the excision of the 2 skin lesions, with no apparent enlargement over the next 7 years, which is highly unlikely for metastatic lesions.

Conclusions

To summarize, the MRI findings of a case of SMA on the floor of the mouth showed low signal intensity on T2WI with a low ADC value and a plateau or persistent signal intensity after rapid initial enhancement on DCE-MRI. These findings are considered characteristic of SMA and reflect the densely fibrous and abundant cellular components of this tumor.

Patient consent

Written informed consent was obtained from the patient for publication of this case report.

REFERENCES

[1] Gordon S, Fischer C, Martin A, Rosman IS, Council ML. Microcystic adnexal carcinoma: a review of the literature. Dermatol Surg 2017;43:1012–16.

[2] Cooper PH. Sclerosing carcinomas of sweat ducts (microcystic adnexal carcinoma). Arch Dermatol 1986;122:261–4.
[3] Cooper PH, Mills SE. Microcystic adnexal carcinoma. J Am Acad Dermatol 1984;10:908–14.
[4] Johnston CA, Toker C. Syringomatous tumors of minor salivary gland origin. Hum Pathol 1982;13:182–4.
[5] Bondi R, Urso C. Syringomatous adenocarcinoma of minor salivary glands. Tumori 1990;76:286–9.
[6] Schipper JH, Holecek BU, Sievers KW. A tumor derived from Ebner's glands: microcystic adnexal carcinoma of the tongue. J Laryngol Otol 1995;109:1211–14.
[7] Closmann JJ, Torske KR. When a mucocele is not a mucocele: adenocarcinoma NOS–a case report and review of the literature. Gen Dent 2007;55:325–7.
[8] Petersson F, Skogvall I, Elmberger G. Sclerosing sweat duct-like carcinoma of the tongue-a case report and a review of the literature. Am J Dermatopathol 2009;31: 691–694.
[9] Basile JR, Lin YL. A salivary gland adenocarcinoma mimicking a microcystic adnexal carcinoma. Oral Surg Oral Med Oral Pathol Oral Radiol Endod 2010;109:e28–33.
[10] Ide F, Kikuchi K, Kusama K. Microcystic adnexal (sclerosing sweat duct) carcinoma of intraoral minor salivary gland origin: an extracutaneous adnexal neoplasm? Oral Surg Oral Med Oral Pathol Oral Radiol Endod 2011;112:284–6.
[11] Mills AM, Policarpio-Nicholas ML, Agaimy A, Wick MR, Mills SE. Sclerosing microcystic adenocarcinoma of the head and neck mucosa: a neoplasm closely resembling microcystic adnexal carcinoma. Head Neck Pathol 2016;10:501–8.
[12] Wood A, Conn BI. Sclerosing microcystic adenocarcinoma of the tongue: a report of 2 further cases and review of the literature. Oral Surg Oral Med Oral Pathol Oral Radiol 2018;125:e94–e102.
[13] Zhang R, Cagaanan A, Hafez GR, Hu R. Sclerosing microcystic adenocarcinoma: report of a rare case and review of literature. Head Neck Pathol 2019;13:215–19.
[14] Zhang L, Huang X, Zhou T, et al. Microcystic adnexal carcinoma: report of rare cases. Biosci Rep 2020:40.
[15] Jiang R, Marquez J, Tower JI, Jacobs D, Chen W, Mehra S, et al. Sequencing of sclerosing microcystic adenocarcinoma identifies mutational burden and somatic variants associated with tumorigenesis. Anticancer Res 2020;40:6375–9.
[16] Tan GZL, Goh GH, Loh KS, Petersson F. Sclerosing microcystic adenocarcinoma of the parotid gland - The first recorded case with histo-cytopathologic correlation and a brief review of the literature. Ann Diagn Pathol 2021;54:151806.
[17] Priya Mathew E, MacMillan CA, Goldstein DP, Smith SM. Primary extraoral sclerosing microcystic adenocarcinoma of the salivary gland. Human Pathol Rep 2021;26:300577.
[18] Lee YY, Hwang TZ, Jin YT, Chen CC. Sclerosing microcystic adenocarcinoma arising from the tongue: a case report and literature review. Diagnostics (Basel) 2022:12.
[19] Board WCoTE Head and neck tumors. Lyon: International Agency for Research on Cancer World Health Organization; 2022.
[20] Rooper LM. Emerging entities in salivary pathology: a practical review of sclerosing microcystic adenocarcinoma, microsecretory adenocarcinoma, and secretory myoepithelial carcinoma. Surg Pathol Clin 2021;14:137–50.
[21] Tawfik AM, Kreft A, Wagner W, Vogl TJ. MRI of a microcystic adnexal carcinoma of the skin mimicking a fibrous tumor: case report and literature review. Br J Radiol 2011;84:e114–17.
[22] Ghorra CS, Naderi S, Zeid SA, Hokayem N, Abboud B. Sublingual gland tumor: do not forget to rule out a metastasis. ANZ J Surg 2010;80:669–70.
[23] Lin Y, Wang Y, Zhang H, August M, Xiang X, Zhang F. Sublingual gland tumors worldwide: a descriptive retrospective study of 839 cases. J Oral Maxillofac Surg 2020;78:1546–56.